ELSEVIER

Agricultural and Forest Meteorology 107 (2001) 207–225

AGRICULTURAL AND FOREST METEOROLOGY

www.elsevier.com/locate/agrformet

Micro-meteorological methods for estimating surface exchange with a disturbed windflow

John D. Wilson [a,*], Thomas K. Flesch [a], Lowry A. Harper [b]

[a] *Department of Earth and Atmospheric Sciences, University of Alberta, Edmonton, Alta., Canada T6G 2E3*
[b] *United States Department of Agriculture, Watkinsville, GA, USA*

Received 18 May 2000; received in revised form 30 November 2000; accepted 1 December 2000

Abstract

This paper examines the accuracy with which trace gas fluxes, from a source that disturbs the local wind and microclimate, may be estimated from measured concentrations, above or downwind from the source. The familiar flux–gradient methods, even if carefully applied within the near-surface constant-flux-layer, nevertheless posit horizontally-uniform wind and stability. Errors result if the windflow is actually advective (i.e. disturbed), so that its state is evolving in the alongwind direction.

We take as an illustration the case of a gas evaporating uniformly (Q, $\mathrm{kg\,m^{-2}\,s^{-1}}$) from a small lagoon. We modify the Rao–Wyngaard–Cote local advection model, verify it against existing observations of disturbed flows, then calculate the fields of windspeed, temperature and tracer concentration over land and lake. From these "data" we calculate several estimates of the (known) source strength Q. Results by integration of the horizontal flux (Q^{IHF}) prove the most satisfactory, followed by those using a source–receptor relationship based on a backward Lagrangian stochastic method (Q^{bLS}). Flux–gradient estimates Q^{FG} can be very seriously in error, and should only be used with caution in disturbed flow. These findings have generality beyond the specific case of a lagoon flow. © 2001 Published by Elsevier Science B.V.

Keywords: Micro-meteorological methods; Disturbed windflow; Local advection; Gas exchange; Trace gas fluxes; Windflow flux-gradient method; Inverse lagrangian method; Atmospheric diffusion; Atmospheric dispersion

1. Introduction

Many natural and artificial components of the landscape emit or absorb gases that impact on the environment, not only locally (e.g. odour), but also at larger scales (e.g. the greenhouse gas methane). Scientists from many disciplines have an interest in the quantification of such exchanges, and it is the purpose of this paper to examine some of the indirect micro-meteorological methods that have been used to that end. We want to emphasize that *spatial variability* of the microclimate, over any distinct portion of the ground, invalidates some of the familiar methods that can be used to measure ground–air gas exchange over uniform surfaces. Flows over swamps or feedlots, landfills or waste lagoons are examples of *disturbed* (or in meteorological jargon, *advective*) flows, whose properties evolve along the direction of the wind. In these cases, if source strength Q is deduced by the application of theories or hypotheses or models whose derivation and validity hinges on the assumption of horizontal-uniformity of the flow, then there are likely to be errors.

To indicate how serious those errors might be, we take as an example a gas evaporated from a small

* Corresponding author. Tel.: +1-780-492-0353.
E-mail address: john.d.wilson@ualberta.ca (J.D. Wilson).

0168-1923/01/$ – see front matter © 2001 Published by Elsevier Science B.V.
PII: S0168-1923(00)00238-0

pond. Our results will thus have direct application to the measurement of fluxes from agricultural waste lagoons, but should also be understood to be general in their implications. We simulate various estimators of the gas flux by first generating *modelled* spatial fields of windspeed, temperature and gas concentration (U, T, C), using a development of the local-advection model of Rao et al. (1974a; hereafter RWC). Both Kroon (1985) and Bink (1996) have used RWC for a similar purpose, viz. to investigate errors in the Bowen-ratio/energy-balance method for determination of surface fluxes of sensible and latent heat in advective flows.

In Section 2 we review the atmospheric surface layer, and the basis of several of the indirect techniques for estimating vertical fluxes (including flux–gradient). In Section 3 we describe the local advection model, and test its performance against observations in measured advective flows (readers not interested in the local advection model may wish to skip this material). Then in Section 4 we use RWC to generate synthetic microclimates for flow over a lagoon, and the accompanying concentration fields of a passive scalar, uniformly released over the lagoon, so as to compare the known source strength Q with that derived from the integrated horizontal flux (Q^{IHF}), from a backward Lagrangian stochastic technique (Q^{bLS}) and from flux–gradient relationships (Q^{FG}).

2. Measuring surface fluxes

The horizontally uniform atmospheric surface layer (ASL) is considered to be a shallow constant stress (and flux) layer, i.e. one generally treats the vertical fluxes of momentum ($\Gamma = -\rho u_*^2$), heat (Q_{H}) and water vapour (E) or latent heat (Q_{E}) as height independent, or better stated, one ignores the fact that they are not (quite). Monin–Obukhov similarity theory (MOST), which is applicable only in the layer $z_0 \ll z \ll \delta$ (where δ is the depth of the atmospheric boundary layer), forms our working framework for this (we emphasize, idealised) flow. MOST can be derived by application of similarity principles to the governing equations, but loosely speaking, we can say that it is based on the judicious selection of characteristic scales. The fluxes themselves provide a velocity scale u_* (the friction velocity) and a temperature scale $T_* = -Q_{\mathrm{H}}/(\rho c_p u_*)$, with corresponding scales for other species (ρ is the air density; c_p is the specific heat capacity of air at constant pressure). The length scale z obviously must be included (whereas z_0 and δ are excluded by restriction of the domain of applicability), as must the buoyancy parameter g/T_0. As a dimensional necessity flowing from these choices, MOST posits for the vertical gradients in mean velocity and temperature the expressions

$$\frac{k_{\mathrm{v}} z}{u_*}\frac{\partial U}{\partial z} = \varphi_{\mathrm{m}}\left(\frac{z}{L}\right) \tag{1}$$

and

$$\frac{k_{\mathrm{vh}} z}{T_*}\frac{\partial T}{\partial z} = \varphi_{\mathrm{h}}\left(\frac{z}{L}\right) \tag{2}$$

(mean values, e.g. of windspeed u, will be denoted interchangeably as $\bar{u}$ or $\langle u\rangle$ or U, while fluctuations from the mean are denoted by a prime: thus $u = \bar{u} + u' = U + u'$, etc.). In Eqs. (1) and (2), k_{v} and k_{vh} are the von Karman constants for momentum and heat (included by convention; more on these below). On the right-hand sides (RHS) appear universal empirical dimensionless functions $(\varphi_{\mathrm{m}}, \varphi_{\mathrm{h}})$ of the ratio z/L of height to the Monin–Obukhov length,

$$L = -\frac{u_*^3}{k_{\mathrm{v}}(g/T_0)(Q_{\mathrm{Hv}}/\rho c_p)} \tag{3}$$

where (again) the factor k_{v} is included by convention (Q_{Hv} is the virtual heat flux, and so incorporates the buoyancy due to water vapour). For a passive tracer emitted at ground with spatially and temporally constant source-strength Q, a concentration scale $C_* = -Q/u_*$ may similarly be defined, and again, the MOST prediction is

$$\frac{k_{\mathrm{vc}} z}{C_*}\frac{\partial C}{\partial z} = \varphi_{\mathrm{c}}\left(\frac{z}{L}\right) \tag{4}$$

We have intentionally distinguished three von Karman constants, i.e. k_{v}, k_{vh}, k_{vc}, because, like Dyer and Bradley (1982), we define the universal functions φ_{m}, φ_{h}, φ_{c} to take unit value in the neutral limit, $|z/L| \to 0$. These MOST expressions imply that the eddy viscosity (K_{m}) and eddy diffusivities for vertical transport of heat (K_{h}) and mass (K) are

$$K_{\mathrm{m}} = \frac{k_{\mathrm{v}} u_* z}{\varphi_{\mathrm{m}}}, \quad K_{\mathrm{h}} = \frac{k_{\mathrm{vh}} u_* z}{\varphi_{\mathrm{h}}}, \quad K = \frac{k_{\mathrm{vc}} u_* z}{\varphi_{\mathrm{c}}} \tag{5}$$

while ratios of the von Karman constants give us the *turbulent* Prandtl and Schmidt numbers,

$$\frac{k_v}{k_{vh}} = Pr = \left(\frac{K_m}{K_h}\right)_{|L|=\infty} \quad (6)$$

and

$$\frac{k_v}{k_{vc}} = Sc = \left(\frac{K_m}{K_c}\right)_{|L|=\infty} \quad (7)$$

There is no reason to suppose the von Karman "constants" actually are constant, across the family of all possible horizontally homogeneous ASL states; for example, Bradshaw (1967) argues that the value of k_v is sensitive to the level of "inactive turbulence". Consequently ratios of von Karman "constants" are also somewhat uncertain, and probably not universal — a point which bears on the accuracy of some of the methods investigated here, and to which we later return.

2.1. Vertical fluxes by eddy-covariance

Suppose we wished to determine the fluxes, Γ or Q_H or Q. Let us start out by supposing stationary, horizontally homogeneous flow over an ideally horizontal, flat, uniform surface (that uniformly releases a gas, whose concentration is $c = c(x, y, z, t)$). The mean vertical eddy flux at a point (x, y, z) over the interval $(t_m - T_{avg}) \leq t \leq t_m$, where T_{avg} is typically 15–60 min, is

$$Q^{EC}(x, y, z, t_m, T_{avg}) = \overline{wc} \quad (8)$$

(the time-average of the turbulent vertical convective mass flux density). By our assumption of symmetry, and neglecting any errors, this vertical flux Q^{EC} equals the flux Q off the source. Potential sources of error in the point eddy flux might include inadequate instrument spectral (temporal) response; inadequate instrument spatial resolution; poor instrument calibration (span, offset); instrument interference with the flow (flow distortion); anemometer-scalar sensor separation; cross-correlated instrument noise; and instrument misalignment relative to the vertical.

But let us assume that of all these possible sources of error, only one arises: we have ideal instrumentation in every respect except that there is or may be an unknown small anemometer offset ϵ. We write for the *measured* vertical velocity

$$w(x, y, z, t) = W(x, y, z, t_m, T) + \varepsilon + w'(x, y, z, t) \quad (9)$$

where we acknowledge explicitly the offset error, ε, and that the (true) mean vertical velocity, W, depends on averaging interval T. Now from the definition above the (apparent) point eddy flux is

$$Q^{EC} = (W + \varepsilon)C + \overline{w'c'} \quad (10)$$

Operationally, however, one recognises the (possible) existence of ε (due to tower misalignment or instrument offset), and the flux normally reported (Q^{ECP}, for "eddy covariance practice") is

$$Q^{ECP} = \overline{wc} - (W + \varepsilon)C = \overline{w'c'} \quad (11)$$

Such fluxes are usually considered to represent surface–air exchange over what are subjectively judged homogeneous surfaces, with the accompanying assumption that if the surface is homogeneous, then so is the atmosphere (which is not necessarily true). More sophisticated "flux corrections" (than the replacement of Eq. (10) by Eq. (11)) are often made in the case that a three-dimensional anemometer has been used, but this does not affect our argument. It is ominous for the credibility of "eddy covariance in practise" that the sum $Q_H + Q_{LE}$ of the sensible and latent heat fluxes, measured by eddy-covariance, not uncommonly fails to match the energy supply ("non-closure" of the surface energy budget; Blanken et al., 1998; Twine et al., 2000).

If the flow is spatially variable, then Eq. (11) for tracer flux is invalid, even if the instruments are placed close enough to ground to be within the constant (gas) flux layer... for flow disturbance almost inevitably introduces a (generally unknown) mean vertical motion W, that may contribute to the local (or spatially averaged) vertical flux of the subject gas (see Finnigan, 2000).

2.2. Vertical fluxes from gradients in uniform conditions

As outlined above, although eddy correlation is regarded as being the most fundamental technique to

measure trace gas exchange fluxes, it is inapplicable in a disturbed flow — and not without ambiguity even in the nominally uniform case (e.g. Mahrt, 1998). Furthermore for many trace gases of interest we lack sufficiently fast concentration sensors. An alternative is to deduce the vertical *flux* by measuring associated vertical mean *gradients*. Such techniques are traditional (and acceptable) in horizontally uniform conditions, but there are potentially grave errors under inhomogeneous conditions.

There are many variations on flux–gradient (FG) techniques, but it will suffice that we examine only one. At an arbitrary location on the x–y plane we select a pair of heights ($z_1 < z_2$), at each of which we measure the mean windspeeds U_1, U_2; the mean temperatures T_1, T_2; and the mean concentrations of the gas C_1, C_2. According to our symmetry assumption — a conceptual idealisation of a reality that is usually more complex — the mean fluxes are absolutely constant, i.e. invariant with x, y, z; and we will have chosen a site so as to attempt to uphold this assumption.

Firstly, we need to know atmospheric stability. We approximate the gradient Richardson number,

$$Ri_g = \frac{(g/T_0)(\partial T/\partial z)}{(\partial U/\partial z)^2} = \frac{k_v}{k_{vh}} \frac{\varphi_h}{\varphi_m^2} \frac{z}{L} \tag{12}$$

(where the expression on the right follows exactly upon substitution for the gradients) as

$$Ri_g = \frac{(g/T_0)\Delta T \Delta z}{\Delta U^2} \tag{13}$$

where $\Delta T = T_2 - T_1$, etc., and the resulting Ri_g is considered to apply at height $z_g = (z_1 z_2)^{1/2}$. As an aside, one will have observed arbitrary decisions entering the picture; the choices z_1, z_2; the use of the geometric mean height. Leaving those issues aside, we exploit an empirical Ri_g versus (z/L) correlation to obtain z_g/L and thus L. There are as many such correlations as there are versions of the universal MOST functions, but as an example (Hogstrom, 1996)

$$\frac{z}{L} = \begin{cases} 0.67 Ri_g, & L < 0 \\ Ri_g(1 - 5Ri_g)^{-1}, & L \geq 0 \end{cases} \tag{14}$$

Any ambiguity or inconsistency or error, e.g. in having ignored that k_v/k_{vh} may not be unity, will to this stage have affected only the value of L we deduce for the flow.

Now, to get the desired flux estimate (which we shall explicitly distinguish from the true flux Q by writing Q^{FG}), we take the ratio of the flux–gradient expressions written above, viz.

$$\frac{Q^{FG}}{u_*^2} = -\frac{k_{vc}}{k_v} \frac{\varphi_m}{\varphi_c} \frac{\Delta C}{\Delta U} \tag{15}$$

where we continue to take pains to admit the possibility that $k_{vc}/k_v \neq 1$. Then by eliminating u_* we obtain:

$$Q^{FG} = -\frac{1}{Sc} k_v^2 \frac{z_g^2}{\Delta z^2} \frac{1}{\varphi_c \varphi_m} \Delta C \Delta U \tag{16}$$

Now, given that the eddy diffusivities (and von Karman constants) are determined from flux–gradient experiments in which (hopefully) correct fluxes are related to correct gradients, it is surely a necessary self-consistency that under situations of suitable horizontal uniformity (of the flow and the scalar sources), Q^{FG} should be a good estimate of Q. Provided we are not too unfortunate or extreme in our choices of z_1, z_2, and if the micro-meteorology of the "uniform" ASL is truly universal and suitably described by MOST, and if the Ri_g–z/L correlation we employed is "true" to MOST, there should be no problem.

Suppose we take the neutral limit; and suppose too we allow z_1 and z_2 to be close together (but we nevertheless assume ideally correct measurements of ΔU, ΔC are obtainable). The expression above simplifies, and the z_g approximation is nearly exact; given that L is of infinite magnitude and so irrelevant in the neutral limit, now only the two von Karman constants k_v, k_{vc} enter the picture. For given measured values of ΔU, ΔC, what we get for our estimate Q^{FG} depends very directly on our choice of those constants,

$$Q^{FG(N)} = -\frac{1}{Sc} k_v^2 \frac{z_g^2}{\Delta z^2} \Delta C \Delta U \tag{17}$$

Dyer and Bradley (1982) concluded from the ITCE flux–gradient experiment that the von Karman constants for humidity, heat and momentum in the atmospheric surface layer were identical, with value 0.4 ± 0.02. Although some (other) flux–gradient experiments have suggested the turbulent Prandtl number (and/or turbulent Schmidt number for vapour) is/are less than unity, many micro-meteorologists treat the eddy viscosity and eddy diffusivities as being identical in the neutral limit — this despite the fact

that in engineering wall shear flows it is near unanimous that they differ.[1] Appendix A discusses some conflicting evidence on these "constants", from which we conclude that, even in ideally uniform conditions, the application of FG methods to determine a source strength is not without uncertainty, or ambiguity.

From Eq. (17) one may infer that the effective mass diffusivity at the intermediate height z_g is implicitly posited to be

$$K_c = \frac{1}{Sc} k_v^2 z_g^2 \frac{\Delta U}{\Delta z} \tag{18}$$

This makes sense in the ideal case considered (neutral, horizontally homogeneous ASL), for which

$$k_v z_g \frac{\Delta U}{\Delta z} = u_* \tag{19}$$

so that the implicit mass diffusivity is $K_c = (1/Sc) k_v z_g u_*$, which is correct, in uniform conditions.

In historical practice, how well has the FG method worked in uniform conditions? The question begs qualification: do we refer to short-term (15–60 min) figures, or to weekly, seasonal or even annual averages; and secondly, what is the standard of comparison, and the uncertainty therein (i.e. how and how well is "true Q" determined)? For *short term* flux–gradient measurements Q^{FG}, one cannot escape stochastic errors that are inherent in flux–gradient relationships. Published "universal" FG relationships are analytical curves fitted to scatter-plots, i.e. correlations of measured data, such as $(z/T^*)(\partial T/\partial z)$ versus z/L. Figs. 1–4 (especially the insets) from Businger et al. (1971), and Figs. 1–3 from Dyer and Bradley (1982), indicate the random scatter, at given z/L, in single (short term) observations of statistics like $(z/T^*)(\partial T/\partial z)$. This scatter amounts, certainly, to no less than about 10% of the mean value — and probably 25% is a more honest figure. Yaglom (1977) emphasises not only this scatter inherent to a given site and given instrumentation, but also the disparity among analytic fits that have been recommended. As Dyer and Bradley concluded, "The evidence is mounting that the atmosphere does not follow the averaged laws at all places and all times even over an excellent site, and the statistical variability of the medium itself must be taken into account". The saving factor is that these stochastic errors, which might be 10 or 20% for any 15–30-min period, should cancel out as we average together increasing numbers of 15 or 30 min estimates (of trace gas fluxes inferred from flux–gradient relationships). And one would argue that if this were not the case — if an FG method did not work in the long term, at an ideal site — well then the site was not ideal, or the measurements were wrong, or (lastly on the scale of probability) MOST is not universal.

Then what is the "bottom line", when estimates Q^{FG} are compared against an independent and reliable standard, at a good site? On considering the spectrum of cases where FG has been subjected to independent verification (e.g. CO_2 tracer experiments, Harper et al., 1973; nitrogen isotopes, Harper et al., 1983), it may be fair to say that error in a (properly executed) FG technique is no worse than error in the standard itself, typically ±15–20%.

2.3. Vertical fluxes from gradients in non-uniform conditions

Now suppose we carry over the above FG technique to the case of emissions from a lagoon (again we emphasize, this is taken as an example of a very general situation). At some distance (x) downstream from the edge of the lagoon we measure at (z_1, z_2), the mean windspeeds U_1, U_2; the mean temperatures T_1, T_2; and the mean concentrations of the gas C_1, C_2. And we apply Eq. (16). What can go wrong?

The first potential problem is that the (true) fluxes $Q(x, z_1)$, $Q(x, z_2)$ at heights z_1, z_2 need not equal the surface flux Q, unless the ratios z_1/x, z_2/x are extremely small, which restriction would put us within the growing "constant flux layer" (or internal boundary layer, IBL) of gas off the source. The second problem is that it is not at all obvious that the inputs ΔU, ΔT have anything useful at all to tell us about Q! In uniform flow, these give us unambiguously the stratification, and parameterize known wind and temperature profiles. But as the wind passes off land

[1] For example, consider Launder (1978) review: "It does not seem possible to write with any certainty on the variation of the turbulent Prandtl/Schmidt number in fully developed pipe and channel flow (p. 271).... It would be helpful to dispel the idea that a turbulent Prandtl number of unity was in any sense the "normal" value... a value of about 0.7 has a far stronger claim to normality (p. 234).... Viewed overall, the weight of experimental evidence seems to suggest that the near-wall value of *Pr* is a little above 0.9 (p. 246)".

and over the lagoon, or whatever other disturbed surface we may consider, adjustments in the wind and temperature profiles occur, and so $(\Delta U, \Delta T)$ from an arbitrary location (upwind? or over the lagoon?) used to fix stability may lead us astray. Under advective conditions then, one is not entitled to expect the familiar similarity relationships between the fluxes and gradients.[2] That crucial fact makes it wrong to expect that the mass diffusivity

$$K_c = \frac{1}{Sc}\frac{k_v z_g}{\varphi_c}\left(\frac{k_v z_g}{\varphi_m}\frac{\Delta U}{\Delta z}\right) \tag{20}$$

implicit in our procedural use of Eq. (16) is a good estimate of the true, unknown mass diffusivity. In Section 4 we shall use synthetic lagoon microclimates (and tracer concentration fields) to quantify the error arising from use of the flux–gradient technique detailed above.

2.4. Mass balance technique

Continuing to suppose a lagoon (or other source) of infinite crosswind (y) extent, there is an exact relationship between the source strength and the upwind–downwind difference in horizontal flux of mass, viz.

$$\int_{x^-}^{x^+} Q\,\mathrm{d}x = \int_{z=0}^{\infty}[(UC + \overline{u'c'})_{x^+} - (UC + \overline{u'c'})_{x^-}]\,\mathrm{d}z \tag{21}$$

where (x^+, x^-), respectively, denote measurement locations (downstream, upstream) from the source, and where no supposition has been made that the emission rate is uniform. If one neglects the contribution of the turbulent flux, then a practical means to approximate Q is to perform measurements so as to approximate the integral:

$$\int_{x^-}^{x^+} Q^{\mathrm{IHF}}\,\mathrm{d}x = \int_{z=0}^{\infty}[(U(x^+, z)C(x^+, z) - U(x^-, z)C(x^-, z)]\,\mathrm{d}z \tag{22}$$

where IHF designates "integrated horizontal flux". It is worth emphasizing that Eq. (21) is theory-independent, and valid irrespective of whether the flow is horizontally homogeneous or disturbed, i.e. no assumption has been made relative to the flow. In the case that the flow is undisturbed, further simplification is valid,

$$\overline{Q^{\mathrm{IHF}}} = \frac{1}{X}\int_{z=0}^{\infty} U(z)[C(x^+, z) - C(x^-, z)]\,\mathrm{d}z \tag{23}$$

where the left-hand side also has been transformed, by the introduction of the mean emission rate over the width (X) of the source. The "background" concentration $C(x^-, z)$ vanishes in many cases.

This technique has been widely used (e.g. Denmead et al., 1977), and studies have shown that neglect of the turbulent flux may not be very serious. It can be generalised to a source of arbitrary geometry, but integration in the crosswind direction (y) is then mandatory — and greatly increases the instrumentation needed. For a source of arbitrary shape, the method of the next section, though predicated on assumptions with respect to the flow, is usually more practical.

2.5. Backward Lagrangian stochastic source–receptor method

Any theory of atmospheric dispersion defines a "source–receptor relationship", i.e. given a source field, and on the basis of some assumptions about (and measurements of) the turbulent flow, it gives an expression for the resultant mean concentration field $\mathbf{C}(\mathbf{x})$. The specific theory might be as simple as a Gaussian plume/puff model (radical oversimplification of the true nature of the flow and of the process of dispersion in the flow), or as complex as the local-advection model described in Section 3, which allows for disturbed flow. But whatever the nature of the theory, one may exploit a given source–receptor relationship to infer Q, from measured concentration C — given (too) some "supporting" information defining the flow.

Flesch et al. (1995) introduced the "backward Lagrangian stochastic" (bLS) source–receptor method, applicable to a source of any geometry. The underlying Lagrangian stochastic-type model (Wilson and Sawford, 1996) is arguably the best available description of turbulent dispersion, and LS models exist *even for disturbed flows* (but of course they do require to be provided the flow statistics, e.g. $U = U(x, y, z)$, $\sigma_w = \sigma_w(x, y, z)$).

[2] Of course these problems do not arise if the fetch over the downwind surface to the instruments is sufficiently large to assure the profiles there are in equilibrium; but then by definition, the situation is not "advective".

As an example of a rigorous application of the bLS method, suppose the flow is horizontally uniform, and that a single surface area source (of arbitrary shape) is emitting a tracer whose background concentration vanishes. To estimate Q one measures the tracer concentration at a single point, C_P, and those variables defining the state of the surface layer (at a minimum, a single wind speed U_{ref} and wind direction; for improved accuracy, also the atmospheric stability, L). The model is applied by generating an ensemble of (N) trajectories from the point P backward in space and time, and where any trajectory touches ground, one records the particle's touchdown position and vertical velocity (x, y, w). An estimate of source strength Q^{bLS} is inferred from those touchdowns as

$$Q^{bLS} = \frac{U_{ref} C_P}{N} \sum \left(\frac{w}{U_{ref}} \right)^{-1} \quad (24)$$

where the summation runs over all touchdowns on the source.

We reiterate that the bLS method does make assumption relative to the flow. Naturally, too, a *good* LS model — tuned to reality — must be used. Our source strengths Q^{bLS} of Section 4 have been derived using Thomson's (1987) multi-dimensional, well-mixed LS model for Gaussian inhomogeneous turbulence, calibrated to Project Prairie Grass (we set $a = 0.5$ which with $\sigma_w/u_* = 1.3$ implies, via Eq. (A.3), that $C_0 \approx 4.8$). But we neglected the *horizontal*-inhomogeneity of the lagoon flow, so ours is therefore a non-rigorous application of the bLS technique.

Section 3 will now describe and test the numerical local advection model that we use to generate the spatial fields of wind, temperature and trace gas concentration over an idealised lagoon, taken as an example of a (mildly) flow-disturbing source. Readers not interested in the details of the advection model may wish to pass directly to Section 4, where we use the model's output fields to test the trace gas flux estimators described above.

3. Modification and testing of a local-advection model

We modified the local advection model of Rao et al. (1974a, b; hereafter RWC) to generate idealised microclimates for testing flux estimators. RWC consists of 16 coupled partial-differential equations, governing all first- and second-order statistical properties of the flow; i.e. mean velocity (U, W), pressure (P), temperature and humidity (T, Q); variances $(\sigma_u^2, \sigma_v^2, \sigma_w^2, \sigma_T^2, \sigma_q^2)$ of the fluctuations (u', v', w', T', q'); covariances (symbolically, $\langle \alpha' \beta' \rangle$), which include the turbulent convective fluxes, such as $\langle w'T' \rangle$; and the turbulent kinetic energy dissipation rate ϵ.

We shall give a very brief discussion of RWC, focusing on developments relative to earlier reports. Stationarity, and symmetry along one spatial axis (y), are assumed; radiative divergences are neglected, and we assume the atmosphere to be unsaturated. The scale of application is the atmospheric surface layer, and so we also neglect the Coriolis force, and treat the flow as being driven by the shear stress Γ, conveniently expressed $\Gamma = -\rho u_*^2$ in terms of a friction velocity u_*, imposed from aloft. One powerful improvement over earlier codes for RWC is that here the mean pressure gradient is not assumed to vanish, or be constant, or otherwise prescribed. In consequence flow obstructions (fences, trees, hills, etc.) that generate a perturbation pressure field can be properly represented.

In "flux" or "transport" form, which is the natural starting point for the numerical method we use, conservation of mean streamwise momentum is expressed by

$$\frac{\partial}{\partial x}(UU + \sigma_u^2) + \frac{\partial}{\partial z}(UW + \overline{u'w'}) = -\frac{\partial P}{\partial x} + S_U \quad (25)$$

Here (U, W) are the mean horizontal (x) and vertical (z) velocities; σ_u^2 is the variance of the alongwind velocity fluctuation; and P is the locally induced mean kinematic pressure departure from a hydrostatic reference state. The final term S_U, which does not normally appear, is a distributed momentum sink, potentially introduced to represent a porous obstacle; e.g. for a long porous fence of height H, mounted at $x = x_F$ normal to the flow,

$$S_U = -k_r U \sqrt{U^2 + V^2 + W^2}\, \delta(x - x_F) s(z - H) \quad (26)$$

where k_r is the dimensionless resistance coefficient of the fence, $\delta(x - x_F)$ is a delta-function specifying the fence stands at x_F, and $s(z, H)$ is a dimensionless unit step function that vanishes above $z = H$ (Wilson, 1985). Please note that upon integration of

Eq. (25) throughout a control volume, a usual step in control volume methods, the step- and delta-functions do nothing other than to select those control volumes in which there is drag, and to identify the velocity acting.

For the vertical velocity W, similarly,

$$\frac{\partial}{\partial x}(UW+\overline{u'w'})+\frac{\partial}{\partial z}(WW+\sigma_w^2) = -\frac{\partial P}{\partial z}+g\frac{T}{T_0}+S_W \tag{27}$$

where T_0 (Kelvin units) is a reference temperature, and T is the mean temperature departure from an adiabatic reference state (properly, T is the potential temperature departure, but the distinction is not important for the shallow layer of these simulations). Conservation of heat is expressed by the statement of non-divergence of the (vector) heat flux,

$$\frac{\partial}{\partial x}(UT+\overline{u'T'})+\frac{\partial}{\partial z}(WT+\overline{w'T'})=0 \tag{28}$$

while statements of identical form express conservation of water vapour and passive tracer.

We shall not detail the closure assumptions, for specification of which we refer the reader to Rao et al. (1974a, b) and Bink (1996). The shear stress equation is

$$\begin{aligned}&\frac{\partial}{\partial x}\left[U\overline{u'w'}-a_t\tau\overline{u'^2}\frac{\partial\overline{u'w'}}{\partial x}\right]\\&\quad+\frac{\partial}{\partial z}\left[W\overline{u'w'}-a_t\tau\overline{w'^2}\frac{\partial\overline{u'w'}}{\partial z}\right]\\&=-\overline{u'w'}\frac{\partial U}{\partial x}-\overline{w'^2}\frac{\partial U}{\partial z}-\overline{u'^2}\frac{\partial W}{\partial x}-\overline{u'w'}\frac{\partial W}{\partial z}\\&\quad+\frac{g}{T_0}(\overline{u'T'}+0.61T_0\overline{u'q'})-c_{13}\frac{\overline{u'w'}}{\tau}\\&\quad+\frac{\partial}{\partial x}\left[a_t\tau\overline{u'w'}\frac{\partial\overline{u'w'}}{\partial z}\right]+\frac{\partial}{\partial z}\left[a_t\tau\overline{u'w'}\frac{\partial\overline{u'w'}}{\partial x}\right]\end{aligned} \tag{29}$$

where $\tau = 2k/\varepsilon$ is a turbulence timescale defined from the turbulent kinetic energy ($k=\frac{1}{2}(\sigma_u^2+\sigma_v^2+\sigma_w^2)$) and its dissipation rate ε. Following RWC we set coefficient $a_t = 0.15$; and we shall later see that the coefficient c_{13} controls the model's von Karman constant for momentum. The corresponding equation for the vertical heat flux has a similar form:

$$\begin{aligned}&\frac{\partial}{\partial x}\left[U\overline{w'T'}-a_t\tau\overline{u'^2}\frac{\partial\overline{w'T'}}{\partial x}\right]\\&\quad+\frac{\partial}{\partial z}\left[W\overline{w'T'}-a_t\tau\overline{w'^2}\frac{\partial\overline{w'T'}}{\partial z}\right]\\&=-\overline{u'w'}\frac{\partial T}{\partial x}-\overline{w'^2}\frac{\partial T}{\partial z}\\&\quad-(1+a_2)\left[\overline{u'T'}\frac{\partial W}{\partial x}-\overline{w'T'}\frac{\partial W}{\partial z}\right]\\&\quad+(1-a_1)\frac{g}{T_0}(\overline{T'^2}+0.61T_0\overline{q'T'})-d_3\frac{\overline{w'T'}}{\tau}\\&\quad+\frac{\partial}{\partial x}\left[a_t\tau\overline{u'w'}\frac{\partial\overline{w'T'}}{\partial z}\right]+\frac{\partial}{\partial z}\left[a_t\tau\overline{u'w'}\frac{\partial\overline{w'T'}}{\partial x}\right]\end{aligned} \tag{30}$$

(coefficients $a_1=\frac{1}{2}$ and $a_2=-\frac{1}{2}$ do not appear in the original work, having been added by Kroon (1985), and thereafter Bink (1996). Finally, the budget of streamwise variance σ_u^2 is modelled as

$$\begin{aligned}&\frac{\partial}{\partial x}\left[U\sigma_u^2-a_t\tau\overline{u'^2}\frac{\partial\sigma_u^2}{\partial x}\right]\\&\quad+\frac{\partial}{\partial z}\left[W\sigma_u^2-a_t\tau\overline{w'^2}\frac{\partial\sigma_u^2}{\partial z}\right]\\&=-2\sigma_u^2\frac{\partial U}{\partial x}-2\overline{u'w'}\frac{\partial U}{\partial z}-\frac{2}{3}\varepsilon-\frac{c_{11}}{\tau}\left(\sigma_u^2-\frac{2}{3}k\right)\\&\quad+\frac{\partial}{\partial x}\left[a_t\tau\overline{u'w'}\frac{\partial\sigma_u^2}{\partial z}\right]+\frac{\partial}{\partial z}\left[a_t\tau\overline{u'w'}\frac{\partial\sigma_u^2}{\partial x}\right]+S_{uu}\end{aligned} \tag{31}$$

where the final term is a kinetic energy sink corresponding to the momentum sinks (S_u, S_w), for a fence having the form (Wilson, 1985)

$$S_{uu}=-4k_r|U|\sigma_u^2\delta(x-x_F)s(z-H) \tag{32}$$

3.1. "Calibration" of the model coefficients relative to reference state

The closure constants are determined analytically by forcing the coupled equations, when reduced to their one-dimensional form (i.e. upon setting $\partial/\partial x = 0$), to reproduce the desired vertical profiles of the flow statistics for a "reference flow". For atmospheric

surface layer models, the natural reference flow is the ideal, horizontally homogenous, *neutrally stratified*, constant stress (and TKE) layer, in local equilibrium (NSL, for short). It is also possible, in principle, to take the *stratified* equilibrium surface layer as the reference state, choosing the closure "constants" so as to enforce ideal MOST profiles of U, T, Q, $\sigma_{u,v,w}$, etc. This is a dubious idea though — for one hopes that the dynamics of the influence of stratification are captured by the equations themselves, through the buoyancy (g/T_0) terms, so that to tune the closure constants that way would be heavy-handed. Therefore like RWC, Kroon and de Bruin (1993), and Bink (1996), we also chose the NSL as the reference state. Consequently, the observables controlling the closure constants are k_v (von Karman's constant); the ratios $c_{uu} = \sigma_u^2/u_*^2$ (and corresponding c_{vv}, c_{ww}) for the NSL; and the equally empirical MOST relationships such as the scalar-variance to (fluctuation-scale)^2 ratio, σ_T^2/T_*^2, etc. There are also more obscure parameters (a, a_1, a_2, b) arising from the closure itself, whose values have not been altered relative to earlier work, i.e. they are calculated within the program, from the above inputs (which we might say are amenable to easy "physical" interpretation), using the NSL limit-form of the governing equations.

Reducing to a horizontally uniform (but still stratified) flow, the shear stress equation is

$$\frac{\partial}{\partial z}\left[-a_t\tau\overline{w'^2}\frac{\partial\overline{u'w'}}{\partial z}\right] = -c_{13}\frac{\overline{u'w'}}{\tau} - \overline{w'^2}\frac{\partial U}{\partial z} + \frac{g}{T_0}(\overline{u'T'} + 0.61T_0\overline{u'q'}) \quad (33)$$

But our idealized surface layer is nominally a constant stress layer, so that the diffusion term (LHS) can be erased. If we were further to adopt MOST to specify the horizontal heat and moisture fluxes, e.g.

$$\overline{u'T'} = c_{us}u_*T_* \quad (34)$$

(etc.) where c_{us} is a constant, then we could rearrange the above into the form of a flux–gradient relationship, with the (modelled) eddy viscosity being — and we stress this interpretation is only valid in the 1D limit — given by

$$K_\mathrm{m} = \frac{\overline{w'^2}\tau}{c_{13}} - \frac{\tau}{c_{13}}\frac{g/T_0}{\partial U/\partial z}c_{us}u_*(T_* + 0.61T_0q_*) \quad (35)$$

Let us progress further to our neutral and uniform reference state. We can erase any term involving g (no buoyancy effects). The TKE dissipation rate is (ideally) $\varepsilon = u_*^3/k_\mathrm{v}z$, while the observed value of k/u_*^2 is slightly variable. The eddy viscosity (Eq. (35)) now reduces to $K_\mathrm{m} = \sigma_w^2\tau/c_{13}$. Clearly then the choice of c_{13}, combined with whatever value we see fit to impose (as applying to the reference state) for k/u_*^2 (a value which impinges on model's K_m through the timescale τ), will control the (model's) von Karman constant. And indeed to ensure that K_m should be equal to the conventional $k_\mathrm{v}u_*z$, it is only necessary to specify $c_{13} = 2c_{ww}k/u_*^2 = c_{ww}(c_{uu} + c_{vv} + c_{ww})$.

A similar simplification of the heat flux equation leads to $K_\mathrm{h} = 1/d_3\sigma_w^2\tau$ for the reference flow, and one is able to specify d_3 to implement in the model whatever value of the turbulent Prandtl number is wanted.

3.2. Addition of a passive tracer

To the equations of the RWC model we added the mass conservation equation for a passive tracer

$$\frac{\partial}{\partial x}(UC + \overline{u'c'}) + \frac{\partial}{\partial z}(WC + \overline{w'c'}) = 0 \quad (36)$$

and, analogous to the RWC treatment of humidity fluxes, for the vertical tracer flux we wrote

$$\frac{\partial}{\partial x}\left[U\overline{w'c'} - a_t\tau\overline{u'^2}\frac{\partial\overline{w'c'}}{\partial x}\right] + \frac{\partial}{\partial z}\left[W\overline{w'c'} - a_t\tau\overline{w'^2}\frac{\partial\overline{w'c'}}{\partial z}\right] = -\overline{u'w'}\frac{\partial C}{\partial x} - \overline{w'^2}\frac{\partial C}{\partial z} - \overline{u'c'}\frac{\partial W}{\partial x} - \overline{w'c'}\frac{\partial W}{\partial z} - d_{3\mathrm{c}}\frac{\overline{w'c'}}{\tau} + \frac{\partial}{\partial x}\left[a_t\tau\overline{u'w'}\frac{\partial\overline{w'c'}}{\partial z}\right] + \frac{\partial}{\partial z}\left[a_t\tau\overline{u'w'}\frac{\partial\overline{w'c'}}{\partial x}\right] \quad (37)$$

(see the RWC equation for $\langle u'q'\rangle$, which has the same form as our $\langle u'c'\rangle$ equation). Here we have introduced a coefficient $d_{3\mathrm{c}}$ which is distinct from its counterpart d_3 in the humidity conservation equation. Evidently by reduction to the neutrally stratified, horizontally uniform reference state, the eddy diffusivity for our passive tracer in that limit is $K_\mathrm{c} = (1/d_{3\mathrm{c}})\sigma_w^2\tau$, and it will now be clear that $c_{13}/d_{3\mathrm{c}}$ is the (model's)

turbulent Schmidt number. As earlier mentioned, we have distinguished d_{3c} for tracer dispersion because tracer experiments, such as Project Prairie Grass, seem to indicate $Sc \approx 0.63$ (Wilson, 1982b), whereas it is widely considered that flux–gradient experiments have established that $Sc = 1$.

3.3. Numerical method

To solve these coupled equations we used Patankar's (1980) SIMPLE(R) method, which makes no simplifying assumption with respect to the pressure field.

Equilibrium (or as they apply to the advection problem, "upwind") properties will be designated by subscript "1", e.g. $U_1(z)$, Γ_1 (the upwind kinematic shear stress), σ_{u1}, etc. Imposed and constant properties for the downstream region are indicated by "2", e.g. in the case of simulations of Bink's arid-moist advection flow, the downstream canopy resistance r_{c2}, or for lagoon simulations the lagoon surface temperature T_{sfc2}.

Typically the flow domain spanned about $-20 \leq x(\mathrm{m}) \leq 100$, with streamwise resolution constant at $\Delta x \approx 1\,\mathrm{m}$. The inflow profiles were calculated as equilibrium solutions (see below) for the upwind surface (inflow temperature and humidity profiles were pinned to specified values T_{ref1}, Q_{ref1} at a reference height z_{ref}), while at the downstream boundary the condition $\partial/\partial x = 0$ was imposed on all variables. The vertical axis spanned about $\max(z_{01}, z_{02}) \leq z \leq 80\,\mathrm{m}$, with resolution Δz constant at about $\Delta z = 0.2\,\mathrm{m}$ below $z = 10\,\mathrm{m}$, and gently increasing above.

Along the upper boundary ($z = z_T$), flow properties were held at their inflow levels for that height (i.e. undisturbed), e.g. $W = 0$, $\langle u'w' \rangle = -u_{*1}^2$ are the upper boundary conditions on W and on U, respectively. Like Kroon and de Bruin (1993) and Bink (1996), we imposed equilibrium MOST values for other properties at the upper boundary, e.g.

$$\overline{u'^2}(z_T) = \varphi_{u2}\left(\frac{z_T}{L_1}\right) u_{*1}^2 \tag{38}$$

where

$$\varphi_{u2}(\xi) = \begin{cases} c_{uu} + 0.2\left(-\dfrac{\xi}{k_v}\right)^{2/3}, & L_1 < 0 \\ c_{uu}, & L_1 > 0 \end{cases} \tag{39}$$

In principle, a less heavy-handed upper boundary condition is that $\partial/\partial z(\sigma_u^2, \text{etc.}) = 0$, but this resulted in equilibrium profiles even less satisfactory than those of Bink (1996). Evidently the closure model is not completely realistic, and in contriving to overcome that deficiency, it helps to impose property values both at ground and aloft.

The lowest gridpoints for U, T, and C lay at location $z_0 + \frac{1}{2}\Delta z$, i.e. above ground, and so flux boundary conditions were needed. The surface momentum flux $\Gamma = \langle u'w' \rangle_{gnd}$ was obtained from the mean windspeed U_P at the lowest U-gridpoint at $z = z_P$, by the usual "wall function" method, i.e.

$$u_* = \frac{k_v U_P}{\ln(z_P/z_0)} \tag{40}$$

where $z_0 = (z_{01}\,\text{or}\,z_{02})$, and $\Gamma = u_*^2 U_P/|U_P|$. From this local friction velocity the surface value for $z\varepsilon$ (which was treated as a compound variable to avoid the severe discretization error that would have arisen in an ε-equation) was specified as $z\varepsilon = u_*^3/k_v$. The surface scalar flux $\langle w'c' \rangle_{gnd} = (0\,\text{or}\,Q)$ was imposed directly. Surface heat and humidity fluxes were specified as follows:

Dryland–moistland advective flow. The upstream (downstream) energy supply $Q_* - Q_G$ was specified and provided a constraint ($Q_* - Q_G = Q_H + Q_E$) on the surface values of Q_H, Q_E upwind (downwind) from the discontinuity at $x = 0$. As the upwind surface (canopy) resistance for moisture flux was unknown, we also specified directly the upwind sensible heat flux density Q_{H1}. Downstream from the surface change, we imposed a known surface resistance r_{c2} in the Penman–Monteith equation for the surface value of the latent heat flux $Q_{E2}(x)$.

Lagoon advective flow. It was not our objective to simulate the flow over any particular real lagoon, to which end we should have had to concern ourselves with such issues as providing proper lower boundary conditions for the air–water interaction (e.g. calculating a spatially variable surface water temperature). Because our purpose was merely to demonstrate plausible advective effects in flow from land over water, we greatly simplified the lower boundary conditions, as have other numerical studies of wind over lakes (e.g. Weisman, 1975).

Momentum and scalar roughness lengths for flow over water vary widely, in relation to the windspeed and the surface state (calm/wavy). According to Garrat (1992; see also Brutsaert, 1982; Fairall et al., 2000)

at low windspeed over an ocean the scalar roughness lengths z_{0h}, z_{0q} for heat and water vapour exceed the momentum roughness length z_0, but at high windspeed the reverse is true. Given the additional complication of the limited fetch over a small pond, rather than dubiously apply available formulations for the ocean, we chose instead to set $z_{0h} = z_{0q} = z_0$. The consequence of that simplification is straightforward: in our simulations the ground/water–air sensible heat exchange flux, for a given value of the ground/water–air temperature difference, is not quite correct (but note from Eq. (41) that this flux varies with the *logarithm* of z_{0h}), and so the rate of adjustment of the temperature profile in the internal boundary layer over the lake is slightly in error, to the extent that we misrepresent $\ln(z_{0h})$.

We specified an upwind value for the Monin–Obukhov length L_1, so that upwind heat flux $Q_{H1} = -\rho c_p u_{*1}^3/(k_v g/T_0 L_1)$ at all z; and we set $Q_{E1} = 0$. Over the lagoon we specified a *constant* surface temperature T_{sfc2}, and specified surface humidity to be the saturation value, $Q = Q^*(T_{sfc2})$. Surface kinematic heat flux at $x > 0$ was calculated as $\langle w'T'\rangle_{02} = -u_* T_*$ from the local friction velocity (see above) and the local temperature scale

$$T_* = \frac{k_v(T_P - T_{sfc2})}{\ln(z_P/z_{02})} \tag{41}$$

implied by the difference $T_P - T_{sfc2}$ between the temperature T_P at the lowest gridpoint and at the lagoon surface (as we noted above, we simplified by writing $z_{0h2} = z_{02}$). An analogous expression determined the local humidity scale q^* and the surface humidity flux $\langle w'q'\rangle$.

3.4. Consistency tests of the local advection model

The equilibrium solutions gave height-independent fluxes of momentum, heat and water vapour (to four significant figures or better), irrespective of the upstream stratification. The corresponding mean profiles $U_1(z)$, $T_1(z)$ and $Q_1(z)$ differed only slightly from standard MOST profiles that (for the purpose of comparison) were generated according to

$$\varphi_m = \left(1 - 28\frac{z}{L}\right)^{-1/4}, \quad \varphi_h = \left(1 - 14\frac{z}{L}\right)^{-1/2}, \quad L \le 0$$
$$\varphi_m = \varphi_h = 1 + 5\frac{z}{L}, \quad L > 0 \tag{42}$$

(Dyer and Bradley, 1982). However, just as was found by Bink (1996), the model's equilibrium profile of σ_u^2 was not in very good agreement with the empirical MOST data.

The initial guess for the spatial fields was (at all x) the equilibrium (inflow) profiles. As a test of the self-consistency of the model, we set $z_{01} = z_{02}$, $Q_{*1} - Q_{G1} = Q_{*2} - Q_{G2}$, etc. (i.e. no change in properties across $x = 0$), and forced the program through 100 cycles; the equilibrium profiles were upheld across the domain to 1 part in 1000 (or better), i.e. no spurious x-wise gradients developed.

3.5. Simulation of an observed dry → moist flow

To ascertain that our implementation of the RWC model performs as well as expected, and can be trusted to generate synthetic microclimates, we simulated previous observations of the mean temperature and humidity fields in windflow from dryland onto irrigated grassland in the La Crau valley (France); see Fig. 1, which may be compared with Bink's (1996; Fig. 6.4a and b) simulation of the same data. These observations are averages over a single 30-min period (Run 42; 22 June 1987, 11:30 h). The highly unstable near-ground temperature profile over the arid upwind plain is rapidly transformed by the growth of a moist, near-neutral internal boundary layer over the cooler, evaporating downwind surface (in other circumstances, a strong inversion develops over the cool surface).

Inputs for our simulation of Run 42 are identical to those used by Bink (1996), given in his Table 6.1. Inflow friction velocity $u_{*1} = 0.63$ m/s and roughness length $z_{01} = 0.01$ m. Reference upwind temperature and specific humidity at $z_{ref} = 3.05$ m were drawn from the observed values on the upwind tower, $T_{ref1} = 24.08^\circ$C and $Q_{ref1} = 0.0066$ (kg/kg), so that Bink's specified temperature and absolute humidity at ($x = 0, z = z_{02}$) were not required. The upstream energy supply was $Q_{*1} - Q_{G1} = 434$ (W m^{-2}), with the upstream sensible heat flux accounting for $Q_{H1} = 362$ (W m^{-2}). Over the downstream surface, $z_{02} = 0.07$ m, and following Bink's observation (his Table 4.4) we set the downstream available energy supply $Q_{*2} - Q_{G2} = 500$ (W m^{-2}). Over the moist surface the canopy resistance $r_{c2} = 47$ (S m^{-1}).

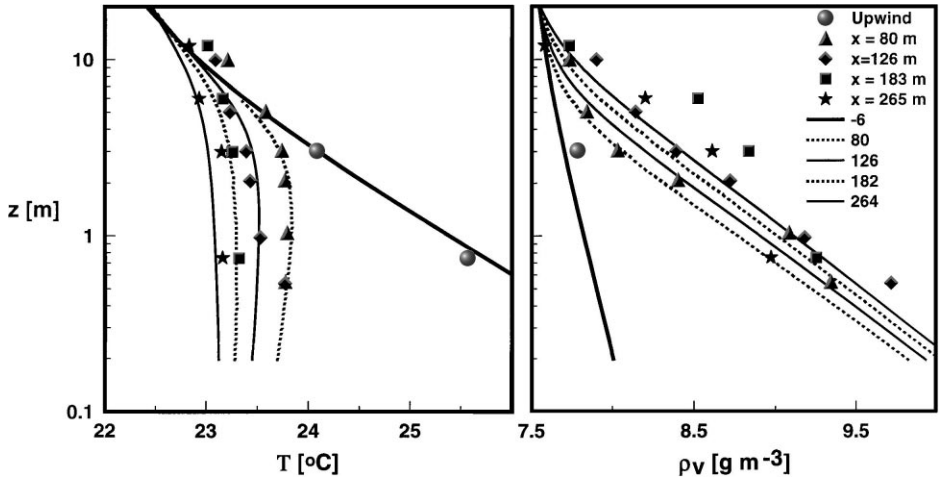

Fig. 1. Observed (symbols) and modelled (lines) vertical profiles of mean temperature and absolute humidity in flow off dryland onto moistland (La Crau Run 42, Bink, 1996).

The good agreement between our solution of the RWC model and the observations only verifies Bink's similar finding, which was achieved using an earlier RWC code. We conclude that RWC captures the primary fields (T, Q) quite well.

3.6. Simulation of an aerodynamically disturbed flow: case of a windbreak

Mean horizontal gradients in the atmospheric surface layer may be generated by changes in the surface boundary fluxes (as in the previous example), by purely aerodynamic disturbances, or by a combination of these influences. We introduced no aerodynamic disturbance in the lagoon flow we use (in the following section) to examine flux estimators, but it is nevertheless useful to make the point that the RWC local advection model handles an aerodynamic disturbance quite as well as it does a change in the boundary fluxes.

Bradley and Mulhearn (1983) reported the distribution of the mean windspeed and shear stress upwind and downwind from a long porous fence, standing nearly perpendicular to the mean wind, in neutrally stratified flow. The height of the fence was $H = 1.2\,\mathrm{m}$, surface roughness length was $z_0 \approx 0.002\,\mathrm{m}$, and the resistance coefficient of the fence was $k_\mathrm{r} = 2$ (measured by Wilson, 1985). Fig. 2 compares the mean wind reduction observed in this experiment and a simulation by the RWC local advection model. The model used $z_{01} = z_{02} (= 0.002\,\mathrm{m})$, $Q_{\mathrm{H1}} \approx Q_{\mathrm{H2}} \approx 0$; the domain spanned $-10 \le x \le 100\,\mathrm{m}$, $z \le 50\,\mathrm{m}$; and gridlengths were $\Delta x = 1\,\mathrm{m}$, $\Delta z = 0.15\,\mathrm{m}$.

Agreement of the modelled mean wind reduction with observations is excellent, indeed more-so than expected from earlier simulations with slightly differing closures and numerical methods (e.g. Wilson and Mooney, 1997). Although we have not shown the

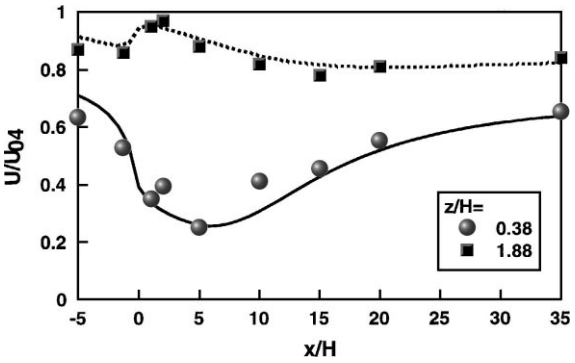

Fig. 2. Solution of the RWC local advection model for mean wind reduction by an infinitely long porous fence in neutrally stratified flow at perpendicular incidence. Symbols give field observations of Bradley and Mulhearn (1983), for the case ($H/z_0 = 600$, $k_\mathrm{r} = 2$), and U_{04} is the mean windspeed observed upstream from the fence at $z = 4\,\mathrm{m}$.

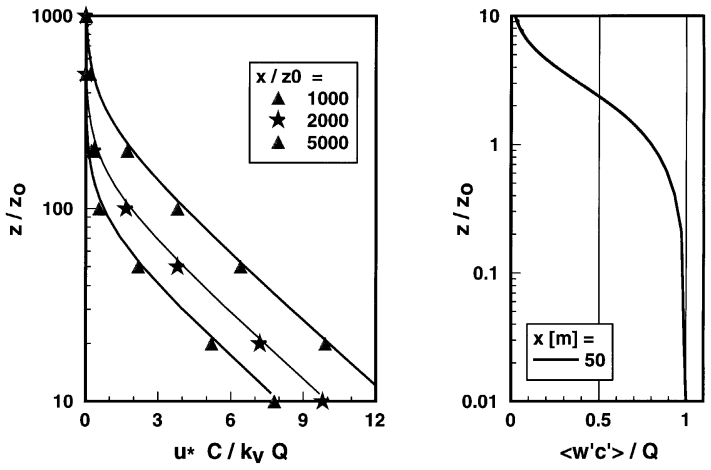

Fig. 3. Vertical profiles of normalised mean concentration u_*C/k_vQ versus distance $x/z_0 = (10^3, 2\times10^3, 5\times10^3)$ downstream from the leading edge of a uniform ground-level area source of strength Q (kg m^{-2} s^{-1}), and profile of mean vertical flux $\langle w'c'\rangle/Q$ at $x/z_0 = 5\times10^3$. Lines give calculations by our local advection model, for conditions of neutrally stratified, horizontally uniform flow with properties: $z_{01} = z_{02} = z_0 = 0.01$ m; $|L_1| = |L_2| = \infty$; $k_v = 0.4$, turbulent Schmidt number $Sc = 0.625$ (normalised profiles are independent of the friction velocity, $u_{*1} = u_{*2} = 0.4$ m s^{-1}, and mean temperature, $T = 25^\circ$C, independent of both x and z). Symbols give the corresponding concentration profiles from a well-mixed Lagrangian stochastic dispersion model, as tabulated in Wilson (1982a; Table II).

modelled TKE field, we found it crucial to include the TKE sink S_{uu} — otherwise the "quiet zone" in the near lee of the windbreak is not captured.

3.7. Verification of the passive tracer dispersion equations in uniform flow

Fig. 3 gives the development of the normalised concentration u_*C/k_vQ and vertical flux $\langle w'c'\rangle/Q$ as a function of z/z_0, for several values of the distance x/z_0 from the leading edge of an area source at ground. Here the local advection model was run with: $z_{01} = z_{02} = z_0 (= 0.01$ m, though the actual value is irrelevant); $|L_1| = 10^3$ m (effectively neutral stratification); $T_{sfc1} = T_{sfc2} = 25^\circ$C; and Schmidt number $Sc = 0.63$. Given neither a roughness change nor a temperature change at $x = 0$, the advection model preserves the incident (approach) flow, so that in effect we have used RWC, supplemented with the passive tracer equations, to simulate dispersion from a surface area source of tracer in the neutral surface layer. The results have been compared with those tabulated by Wilson (1982a) for this same case (his Table II). Those results stem from a one-dimensional Lagrangian stochastic (LS) trajectory model, which was subsequently proven (Thomson, 1987) to be the unique, well-mixed model for Gaussian inhomogeneous turbulence. The LS model had been calibrated (see Appendix A) against the Project Prairie Grass experiments on short range dispersion, and so we therefore regard the concentration profiles of Fig. 3 as being essentially "true."

We have seen that the RWC closure reduces effectively to K-theory in the 1D limit. It is also the case that the LS model, though more general than K-theory, gives results *equivalent* to K-theory for surface sources. Thus it should not be surprising that the two models compared on Fig. 3 have given such close results — this is only an expected and necessary self-consistency. We need not unduly worry about the small differences. Numerical parameters come into play (e.g. grid spacing in the Eulerian model), and furthermore, RWC includes u' (and its correlation with w'), whereas the Wilson (1982a) LS model neglected the streamwise fluctuation.

This section has provided evidence that our augmented RWC model is competent to generate credible profiles of windspeed, temperature and tracer concentration within highly disturbed surface layer flows. We reiterate that, for better or worse, all dispersion models need to be calibrated against observations; and that, by the criterion of Project Prairie Grass, the best calibration for RWC is to set $Sc = 0.63$.

Table 1
Character of the simulated lagoon flows, and the quality (Q^{est}/Q) of various estimators ($Q^{est} = Q^{FG}$, Q^{IHF} or Q^{bLS}) of the lagoon emission rate, derived from the synthetic concentration profile at $x = 50$ m. For the FG method, z_1, z_2 specify the measurement levels; for the bLS method, up (or down) means trajectories were calculated assuming a horizontally uniform atmosphere whose properties are those derived from the upwind (or over-lagoon, $x = 50$ m) profiles of mean windspeed and temperature

Lagoon	Upwind			Downwind			Flux–gradient			IHF	BLS	
	z_0 (m)	T_{up}(°C)	L (m)	z_0 (m)	T_{lag}(°C)	L (m)	$z_1 = 0.14$, $z_2 = 0.39$	$z_1 = 0.39$, $z_2 = 0.64$	$z_1 = 0.39$, $z_2 = 1.39$		Up	Down
A	0.01	25	−23	0.001	25	−12	0.91	0.78	0.72	1.09	0.77	0.89
B	0.01	25	−23	0.001	30	−7	0.94	0.83	0.79	1.08	0.77	0.92
C	0.01	25	−23	0.001	20	−27	0.85	0.71	0.63	1.10	0.77	0.90
D	0.01	25	−23	0.001	15	103	0.82	0.62	0.52	1.09	0.77	0.88
E	0.01	25	48	0.001	25	23	0.61	0.43	0.36	1.03	0.71	0.86
F	0.01	25	48	0.001	30	−22	0.69	0.56	0.53	1.03	0.71	0.88
G	0.01	25	48	0.001	20	6	0.51	0.29	0.19	1.03	0.72	0.96
H	0.01	25	48	0.001	15	2	0.43	0.18	0.09	1.03	0.72	1.44
I	0.01	20	−2300	0.001	30	−6	0.92	0.86	0.85	1.05	0.78	0.97
J	0.01	20	−2300	0.001	10	5	0.61	0.37	0.23	1.06	0.79	1.03

4. Estimates of lagoon emissions in a synthetic lagoon flow

In Section 3 we described a local advection model that we showed does a plausible job of calculating disturbed microclimates (mean wind, temperature and humidity, as well as statistics of the turbulence), and that gives correct results for tracer dispersion in horizontally homogeneous flows. We have used that model to calculate the spatial fields of U, T and C over an idealised lagoon, and applied the flux–gradient technique (Eq. (16)) and other flux estimators (Q^{IHF}, Q^{bLS}) to that synthetic data, to derive estimates of the tracer source strength that can be compared with the independently known source strength (Q; constant over the source, and zero outside its boundaries).

Table 1 documents the cases simulated, which cover a range in stability of the approaching flow (very unstable, neutral, very stable), and specify a (fixed) lagoon surface temperature T_{sfc2} that (in many cases) differs greatly from the surface temperature T_{sfc1} of the approach flow. In all cases, roughness lengths were $z_{01} = 0.01$ m, $z_{02} = 0.001$ m (with no change in elevation of the surface). In those cases where upstream and downstream surface temperatures are equal, of course whatever development does occur is attributable to the roughness change, and evaporation from the lagoon. We made no attempt to replicate observed microclimates over any particular lagoon — in a real case we should have had the complication of terrain to deal with (a berm, or a change in level), and (possibly) variable lagoon temperature and gas emission rate.

To calculate the synthetic tracer concentration field due to emission by the lagoon, in the RWC model we set the turbulent Schmidt number $Sc = 0.63$, the value required for best agreement with Project Prairie Grass.

Fig. 4a and b give the calculated profiles of U, T upstream and at various distances over the lagoon, for cases D (unstable → stable), and F (stable → unstable). Upstream–downstream changes in the U, T profiles can be large, leading to changes in magnitude (and even sign) of L for the upstream or downstream profiles, implying a consequent ambiguity for methods such as FG.

4.1. Comparison of estimates of the tracer flux Q by various techniques

Table 1 and Fig. 5 compare several estimates of the source strength (emission rate from the lagoon). In all cases the FG formula (Eq. (16)) was applied with $Sc = 0.63$ (the value assumed to generate the synthetic data). Please note however, that users of FG might presuppose $Sc = 1$, which may not be correct — in which case their estimates Q^{FG} will contain an error in addition to that (Table 1) having neglected the advective character of the flow.

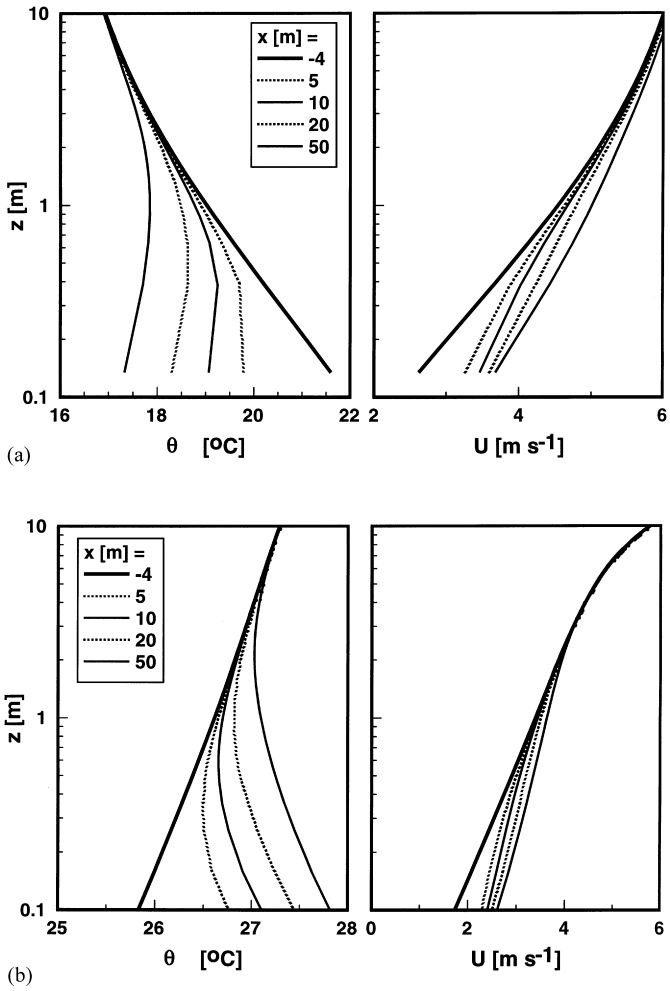

Fig. 4. Evolution of mean temperature and velocity fields in flow off land onto a lagoon, as calculated by the local advection model. (a) Case D, unstable approaching flow encounters a cold lagoon, causing development of a stable internal boundary layer (inversion). (b) Case F, stable approaching flow encounters a warm lagoon, causing development of an unstable internal boundary layer.

The FG method exploits differences in U, T, C between two heights (z_1, z_2) at $x = 50\,\mathrm{m}$. From Table 1 we see that in the case of a stable approach flow, and the more-so in the IBL over a cold lagoon (so that the developing IBL is even more strongly stably stratified than the approach flow), it is necessary to ensure that both observation levels (z_1, z_2) lie very close to the lagoon surface — because the downstream "fully adjusted" or "constant-flux" layer develops very slowly. In the worst (seen) case, $Q^{\mathrm{FG}}/Q < 0.1$, i.e. the flux–gradient method is quite unacceptable. And even when FG is applied using a pair of levels very close to the lagoon surface ($z_1 = 0.14\,\mathrm{m}$, $z_2 = 0.4\,\mathrm{m}$), errors of order 50% can easily occur in stable approach flow.

Integrated horizontal flux (IHF) estimates Q^{IHF} of the source strength, also given in Table 1, were produced by a height integration of the (model's) streamwise flux,

$$Q^{\mathrm{IHF}} = \sum_j U_j C_j \Delta z \tag{43}$$

i.e. the contribution of the turbulent flux was neglected, as it usually is in field implementation of the IHF method. Of course errors due to the need to

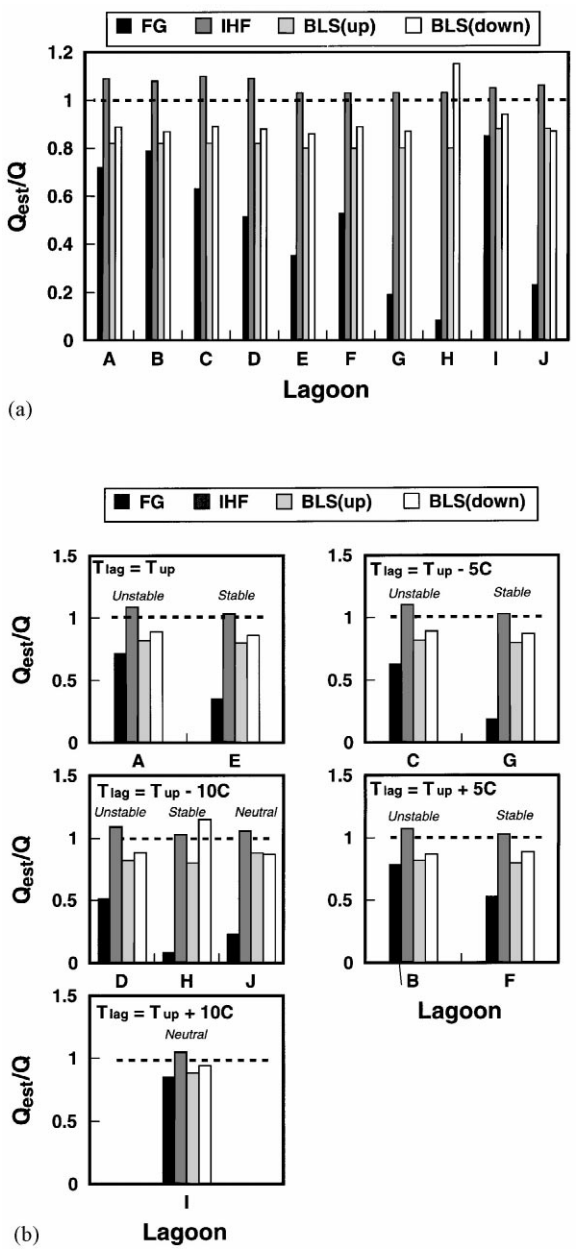

Fig. 5. Comparison of various estimators ($Q_{\mathrm{est}} = Q^{\mathrm{FG}}$, Q^{IHF} or Q^{bLS}) of the known tracer flux Q emitted by the lagoon, by analysis of a synthetic experiment using the local advection model, covering the situations given in Table 1. Figures for Q^{FG} are for $z_1 = 0.39$, $z_2 = 1.39\,\mathrm{m}$.

extrapolate above and below instrumentation levels do not occur in this synthetic case, but, clearly the IHF method is very satisfactory.

The Q^{bLS} estimates derive from a single (synthetic) concentration C_{P} measured at $x = 50\,\mathrm{m}$, $z = 1.4\,\mathrm{m}$, over the lagoon. Backward trajectories from that point were calculated, assuming a horizontally uniform wind field consistent with measured properties either upwind, or (at $x = 50\,\mathrm{m}$) over the lagoon (as indicated earlier, the LS model, which is multi-dimensional, was calibrated to Project Prairie Grass by setting $a = 0.5$). Evidently, despite the fact that the bLS model neglected flow inhomogeneity, it gives better estimates of Q in our synthetic experiment than does the FG method.

5. Conclusion

We have not attempted to deduce from these results any systematic correction factor for the flux–gradient method, for that would require consideration be given to many other factors (e.g. most obviously, the fetch x over the lagoon). Indeed, we are uncertain whether the range of cases we studied is realistic — in terms of approach stability, our "extreme stabilities" are in fact not very extreme. It is clear enough that bad errors[3] can occur when using the FG technique in advective conditions, and so great caution in its use is mandatory, and on the evidence presented, other methods (Q^{bLS}, Q^{IHF}) are preferable.

Of these, the IHF method is attractive from the point of view of being theory-independent (and, but for neglect of the turbulent alongwind flux, assumption free). However even for a situation involving y-symmetry, IHF demands measurement of C at several points (to define the integral, Eq. (23)), and without such symmetry, IHF is impractical. In contrast bLS, though not "assumption free", requires only a single concentration measurement (two, if background concentration is non-zero), is applicable to any source geometry whatsoever — and on the evidence presented, gives rather satisfactory estimates of Q even when one

[3] For some lagoon gases, e.g. ammonia, daytime fluxes far exceed those during the night, when windspeed and lagoon surface temperature are lower; in such circumstances daily and longer-term flux estimates based on FG may be satisfactory.

neglects flow changes. Had we taken the trouble to adopt an LS model that admits horizontal inhomogeneity, and "fed" it with the disturbed flow properties generated by the advection model, we should perhaps have had near perfect agreement, $Q^{\mathrm{bLS}} = Q$.

One can argue that since the local-advection model here has been the criterion for these various flux-estimators, perhaps the best solution is to employ the source–receptor relationship implicit in that model. In principle this is a good idea,[4] however, it would entail treating the lagoon emission problem as what it (really) is — a disturbed flow, demanding numerous measurements to provide the needed suite of (flow) boundary conditions. Furthermore, on a real lagoon Q may not be spatially constant, a factor the local advection model cannot easily handle, unless modified to provide the proper physical and chemical feedbacks operating at the water–air boundary.

Finally we want it to be very clear that, although we have taken the estimation of lagoon emissions as our case in point, these findings with respect to methodology in flux estimation are absolutely general in their scope.

Acknowledgements

The financial support of the Natural Sciences and Engineering Research Council of Canada (NSERC) is acknowledged. The opportunity to study and implement the Rao–Wyngaard–Cote local advection model arose during JDW's sabbatical visit with Drs. Keith McNaughton and Johannes Laubach, at Hort+Research, Kerikeri, New Zealand. We thank Dr. Niek Bink for his helpful comments on his experience with RWC and the La Crau experiments.

[4] It is pertinent to quote Finnigan (2000): "We should not expect... to close scalar budgets in 2D or 3D flow fields, when we only have measurements at a single point. The alternatives are to work at a topographically ideal site and accept the intrinsic limits to accuracy imposed by the stochastic character of atmospheric flow or if one's site is less than ideal, undertake the modelling and more intensive measurements needed to characterise the flow patterns peculiar to that site..." We also paraphrase a comment by Dr. Finnigan at the 24th Conference of the American Meteorological Society on Agricultural and Forest Meteorology (August 2000; Davis, CA, USA) to the effect that the best prospect for immunization of vertical flux estimates from tall towers (such as CO_2 fluxes of the Ameriflux network) against errors due to oversimplification of the flow will be to blend the vertical flux measurements with other necessary data (e.g. steamwise concentration gradients) using a flow *model*.

Appendix A. The von Karman constants, and their relationship with "calibration" coefficients of dispersion models

We have already noted that atmospheric "flux–gradient" experiments are not unanimous on the values of the von Karman constants for momentum, heat and vapour. An alternative and indirect source of information upon them stems from atmospheric tracer experiments.

Hassid (1983) and Wilson (1982b) have noted that the Schmidt number imposed in (at least some types of) Eulerian dispersion models must differ from unity, in order to attain best simulations of reliable tracer experiments such as Project Prairie Grass (PPG). More specifically, Eulerian dispersion models whose form reduces (in the limit of undisturbed, horizontally uniform flow) to

$$U\frac{\partial C}{\partial x} = \frac{\partial}{\partial z}\left(K(z)\frac{\partial C}{\partial z}\right) \tag{A.1}$$

with $K \propto \sigma_w^2$ apparently require $K_c/K_m \approx 1.6$ (i.e. $Sc \approx 0.63$) for optimal agreement with the observations. As is indicated in Section 3, the (extended) Rao–Wyngaard–Cote second-order closure model, used in Section 4 to generate lagoon microclimates, falls within this category.

In modern Lagrangian stochastic (LS) simulations of dispersion (Wilson and Sawford, 1996) a universal constant C_0 appears, whose prescription is equivalent to the prescription of Sc in a K-theory model, because a Lagrangian model implies an underlying diffusion model in the "diffusion limit" (Durbin, 1984). For example, Thomson's (1987) well-mixed multi-dimensional LS model for Gaussian turbulence, which we used for the "backward LS" estimates Q^{bLS} of lagoon emission rate, implies in the diffusion limit an eddy diffusivity

$$K = \frac{2(\sigma_w^4 + u_*^4)}{C_0\varepsilon} \tag{A.2}$$

for vertical diffusion in the neutral surface layer (Sawford and Guest, 1988). This diffusivity may be related

to an *effective* Lagrangian decorrelation timescale T_L, by defining $K = \sigma_w^2 T_L$. It has been common in LS models of the neutral ASL to write $T_L = az/\sigma_w$, thus $K = a\sigma_w z$. In view of Eq. (A.2), and if we assume the TKE dissipation rate $\varepsilon = u_*^3/k_v z$, the relationship between C_0 and the empirical coefficient a is

$$C_0 = \frac{2k_v}{a}\frac{c_w^4 + 1}{c_w} \tag{A.3}$$

where $c_w = \sigma_w/u_*$.

The 1D form of Thomson's model is the *unique* well-mixed first-order LS model for *vertical* diffusion in the ASL, i.e. is the correct model if fluctuations of a particle's horizontal velocity away from the local mean $\bar{u}(z)$, $\bar{v}(z)$ are ignored (this because it proves adequate to specify the velocity PDFs of the ASL as Gaussian). The diffusion limit for the 1D model is obtained by dropping the factor u_*^4 from Eq. (A.2) and (correspondingly) the factor "1" from Eq. (A.3).

One may evaluate C_0 (and thus, through Eq. (A.2)) the Schmidt number *Sc*, by requiring that an LS model best reproduce observations of tracer dispersion (e.g. Du et al., 1995). Wilson et al. (1981) "calibrated" the one-dimensional form of Thomson's LS model (particle velocity vector $\bar{u}$, $\bar{v}$, w) against Project Prairie Grass, by tuning the formula $T_L = az/\sigma_w$. They recommended $a \approx 0.5$, which implies $Sc \approx 0.63$, and (using (A.2) with the term u_*^4 neglected) $C_0 \approx 3.1$ (if $\sigma_w/u_* = 1.25$), or $C_0 = 3.5$ (if $\sigma_w/u_* = 1.3$). Wilson et al. (1984) also found $a \approx 0.5$ a suitable choice, in comparing the 1D LS model with a tracer dispersion experiment on a beach in New Zealand.

Best agreement of PPG with the *multi-dimensional* Thomson model is still procured with $a \approx 0.5$, implying $Sc \approx 0.63$. The corresponding C_0 is larger than estimates from a 1D model, namely $C_0 \approx 4.4$ (if $\sigma_w/u_* = 1.25$) or $C_0 = 4.8$ (if $\sigma_w/u_* = 1.3$). Estimates from direct numerical simulations (Sawford and Yeung, 2000) suggest even larger values of $C_0 \approx 6$–7.

References

Bink, N.J., 1996. The structure of the atmospheric surface layer subject to local advection. Ph.D. Thesis. Wageningen Agricultural University, 206 pp. ISBN 90-5485-513-4.

Blanken, P.D., Black, T.A., Neumann, H.H., den Hartog, G., Yang, P.C., Nesic, Z., Staebler, R., Chen, W., Novak, M.D., 1998. Turbulent flux measurements above and below the overstory of a boreal aspen forest. Bound. Layer Meteorol. 89, 109–140.

Bradley, E.F., Mulhearn, P.J., 1983. Development of velocity and shear stress distributions in the wake of a porous shelter fence. J. Wind Eng. Indust. Aerodyn. 15, 145–156.

Bradshaw, P., 1967. 'Inactive' motion and pressure fluctuations in turbulent boundary layers. J. Fluid Mech. 30, 241–258.

Brutsaert, W., 1982. Evaporation into the Atmosphere. Theory, History and Applications. Reidel, Dordrecht. ISBN 90-277-1247-6.

Businger, J.A., Wyngaard, J.C., Izumi, Y., Bradley, E.F., 1971. Flux-profile relationships in the atmospheric surface layer. J. Atmos. Sci. 28, 181–189.

Denmead, O.T., Simpson, J.R., Freney, J.R., 1977. A direct field measurement of ammonia emission after injection of anhydrous ammonia. Soil Sci. Soc. Am. J. 41, 1001–1004.

Du, S., Sawford, B.L., Wilson, J.D., Wilson, D.J., 1995. A determination of the Kolmogorov constant (C_0) for the Lagrangian velocity structure function, using a second-order Lagrangian stochastic model for decaying homogeneous, isotropic turbulence. Phys. Fluids 7, 3083–3090.

Durbin, P.A., 1984. Comments on papers by Wilson et al. (1981) and Legg and Raupach (1982). Bound. Layer Meteorol. 29, 409–411.

Dyer, A.J., Bradley, E.F., 1982. An alternative analysis of flux-gradient relationships at the 1976 ITCE. Bound layer Meteorol. 22, 3–19.

Fairall, C.W., Hare, J.E., Edson, J.B., McGillis, W., 2000. Parametrization and micrometeorological measurement of air–sea gas transfer. Bound. Layer Meteorol. 96, 63–105.

Flesch, T.K., Wilson, J.D., Yee, E., 1995. Backward-time Lagrangian stochastic dispersion models, and their application to estimate gaseous emissions. J. Appl. Meteorol. 34, 1320–1332.

Finnigan, J.J., 2000. A comment on the paper by Lee (1998): on micrometeorological observations of surface–air exchange over tall vegetation. Agric. For. Meteorol. 97, 55–64.

Garrat, J.R., 1992. The Atmospheric Boundary Layer. Cambridge University Press, Cambridge. ISBN 0-521-38052-9.

Harper, L.A., Box Jr., J.E., Baker, D.N., Hesketh, J.D., 1973. Carbon dioxide and the photosynthesis of field crops. A tracer examination of turbulent transfer theory. Agron. J. 65, 574–578.

Harper, L.A., Catchpoole, V.R., Vallis, I., 1983. Ammonia loss from fertilizer nitrogen applied to tropical pastures. In: Freney, J.R., Simpson, J.R. (Eds.), Gaseous Loss of Nitrogen from Plant–Soil Systems. Nijhoff, The Hague, pp. 195–214.

Hassid, S., 1983. Turbulent Schmidt number for diffusion models in the neutral boundary layer. Atmos. Environ. 17, 523–527.

Hogstrom, U., 1996. Review of some basic characteristics of the atmospheric surface layer. Bound. Layer Meteorol. 78, 215–246.

Kroon, L.J.M., 1985. Profile derived fluxes over inhomogeneous terrain: a numerical approach. Ph.D. Thesis. Wageningen Agricultural University, 159 pp.

Kroon, L.J.M., de Bruin, H.A.R., 1993. Atmosphere–vegetation interaction in local advection conditions: effect of lower boundary conditions. Agric. For. Meteorol. 64, 1–28.

Launder, B.E., 1978. Heat and mass transport. In: Bradshaw, P. (Ed.), Topics in Applied Physics, Vol. 12, Turbulence. Springer, Berlin (Chapter 6).

Mahrt, L., 1998. Flux sampling errors for aircraft and towers. J. Atmos. Ocean. Technol. 15, 416–429.

Patankar, S.V., 1980. Numerical heat transfer and fluid flow. Series in computational methods in mechanics and thermal sciences, Hemisphere Publishing Co., London.

Rao, K.S., Wyngaard, J.C., Cote, O.R., 1974a. Local advection of momentum, heat, and moisture in micrometeorology. Bound. Layer Meteorol. 7, 331–348.

Rao, K.S., Wyngaard, J.C., Cote, O.R., 1974b. The structure of the two-dimensional internal boundary layer over a sudden change of surface roughness. J. Atmos. Sci. 31, 738–746.

Sawford, B.L., Guest, F.M., 1988. Uniqueness and universality in Lagrangian stochastic models of turbulent dispersion. In: Preprints of the Eighth Symposium on Turbulence and Diffusion, American Meteorological Society, Boston, p. 96.

Sawford, B.L., Yeung, P.K., 2000. Eulerian acceleration statistics as a discriminator between Lagrangian stochastic models in uniform shear flow. Phys. Fluids 12, 2033.

Thomson, D.J., 1987. Criteria for the selection of stochastic models of particle trajectories in turbulent flows. J. Fluid Mech. 180, 529–556.

Twine, T.E., Kustas, W.P., Norman, J.M., Cook, D.R., Houser, P.R., Meyers, T.P., Prueger, J.H., Starks, P.J., Wesley, M.L., 2000. Correcting eddy-covariance flux underestimates over a grassland. Agric. For. Meteorol. 103, 279–300.

Weisman, R.N., 1975. A developing boundary layer over an evaporating surface. Bound. Layer Meteorol. 8, 437–445.

Wilson, J.D., 1982a. Turbulent dispersion in the atmospheric surface-layer. Bound. Layer Meteorol. 22, 399–420.

Wilson, J.D., 1982b. An approximate analytical solution to the diffusion equation for short range dispersion from a continuous ground-level source. Bound. Layer Meteorol. 23, 85–103.

Wilson, J.D., 1985. Numerical studies of flow through a windbreak. J. Wind Eng. Indust. Aero. 21, 119–154.

Wilson, J.D., Mooney, C.J., 1997. In: Wang, H., Takle, E. (Eds.), Comments on ‘a numerical simulation of boundary-layer flows near shelterbelts’. Bound. Layer Meteorol. 85, 137–149.

Wilson, J.D., Sawford, B.L., 1996. Lagrangian stochastic models for trajectories in the turbulent atmosphere. Bound. Layer Meteorol. 78, 191–210.

Wilson, J.D., Thurtell, G.W., Kidd, G.E., 1981. Numerical simulation of particle trajectories in inhomogeneous turbulence. III. Comparison of predictions with experimental data for the atmospheric surface-layer. Bound. Layer Meteorol. 21, 443–463.

Wilson, J.D., Clarkson, T.S., Hadfield, M.D., 1984. Observations of wind flow and tracer-gas dispersion over sand dunes. NZ J. Sci. 27, 237–242.

Yaglom, A.M., 1977. Comments on wind and temperature flux-profile relationships. Bound. Layer Meteorol. 11, 89–102.